

# Supporting Information for: Optimization of Potential Non-covalent Inhibitors for SARS-CoV-2 Main Protease Inspected by a Descriptor of Subpocket Occupancy

Yujia Sun <sup>a</sup>, Bodi Zhao <sup>a</sup>, Yuqi Wang <sup>a</sup>, Zitong Chen <sup>a</sup>, Huaiyu Zhang <sup>b</sup>, Lingbo Qu <sup>a</sup>, Yuan Zhao <sup>\*c</sup>, Jinshuai Song <sup>\*a</sup>

<sup>a</sup> Green Catalysis Center, and College of Chemistry, Zhengzhou University, No. 100 Science Avenue, Zhengzhou, Henan 450001, P. R. China

<sup>b</sup> Institute of Computational Quantum Chemistry, College of Chemistry and Materials Science, Hebei Normal University, Shijiazhuang, Hebei 050024, P. R. China

<sup>c</sup> The Key Laboratory of Natural Medicine and Immuno-Engineering, Henan University, Kaifeng, Henan 475000, P. R. China

E-mail: [jssong@zzu.edu.cn](mailto:jssong@zzu.edu.cn); [zhaoyuan@henu.edu.cn](mailto:zhaoyuan@henu.edu.cn)

## Content

Supporting Information for: Simulation and optimization of potential non-covalent inhibitor for SARS-CoV-2 Main Protease .....	1
Part 1: Functions of 13 Marketed Drugs .....	2
Part 2: Docking Results .....	3
Part 3: Molecular Dynamics Simulations Results and Free-Energy Calculations .....	5
Part 4: Physicochemical properties and ADME analysis .....	20
Part 5: Simplified Molecular Input Line Entry System .....	22

## Part1: Functions of 13 Marketed Drugs

Adrafinil, a psychostimulant that activates the postsynaptic  $\alpha 1$  adrenergic receptors of the central nervous system. Bromefric acid, a medicine for the treatment of neurological disorders. Fusidic acid is an antibiotic with steroidal skeleton, which is highly sensitive to various gram-positive cocci, especially staphylococci. LSN-2463359 is a positive allosteric modulator of metabotropic glutamate 5 (mGlu5), which can attenuate behavioral response after the administration of competitive NMDA receptor antagonists. MUT056399 is a highly potent inhibitor of the FabI enzyme of both *Staphylococcus aureus* and *Escherichia coli*. Necrostatin-1 (Nec-1) effectively inhibits TNF $\alpha$ -induced necrotic death of L929 cells and prevents radiocontrast media (RCM)-induced dilation of peritubular capillaries. Nec-1 is a potent necroptosis inhibitor, RIP1 kinase inhibitor and IDO inhibitor. Polydatin, the glycoside of Resveratrol, can inhibit ICAM-1 expression, elevate  $Ca^{2+}$ , weaken white blood cell–endothelial cell adhesion, and activate KATP channels in the myocardial cell, white blood cell, vascular smooth muscle cell, and endothelial cell. SEN-1269, a novel inhibitor of amyloid-beta toxicity. AZD6482 is a selective inhibitor that blocks the interaction of ATP with PI3K $\beta$  and inhibits platelet aggregation induced by low concentrations of agonists. SUN-B-8155 is a non–peptide agonist of the calcitonin receptor which selectively mimics the biological effects of calcitonin. Clonidine is an alpha 2-adrenergic agonist and it can suppress the firing activity of neurons. UNC2327 is an allosteric inhibitor of protein arginine methyltransferase 3 (PRMT3). Tretazicar, an antitumor prodrug, is highly selective against the Walker 256 rat tumour line which has sensitivity for retrovirally transduced AB22 (AB22-nr) cells.

## Part 2: Docking Results

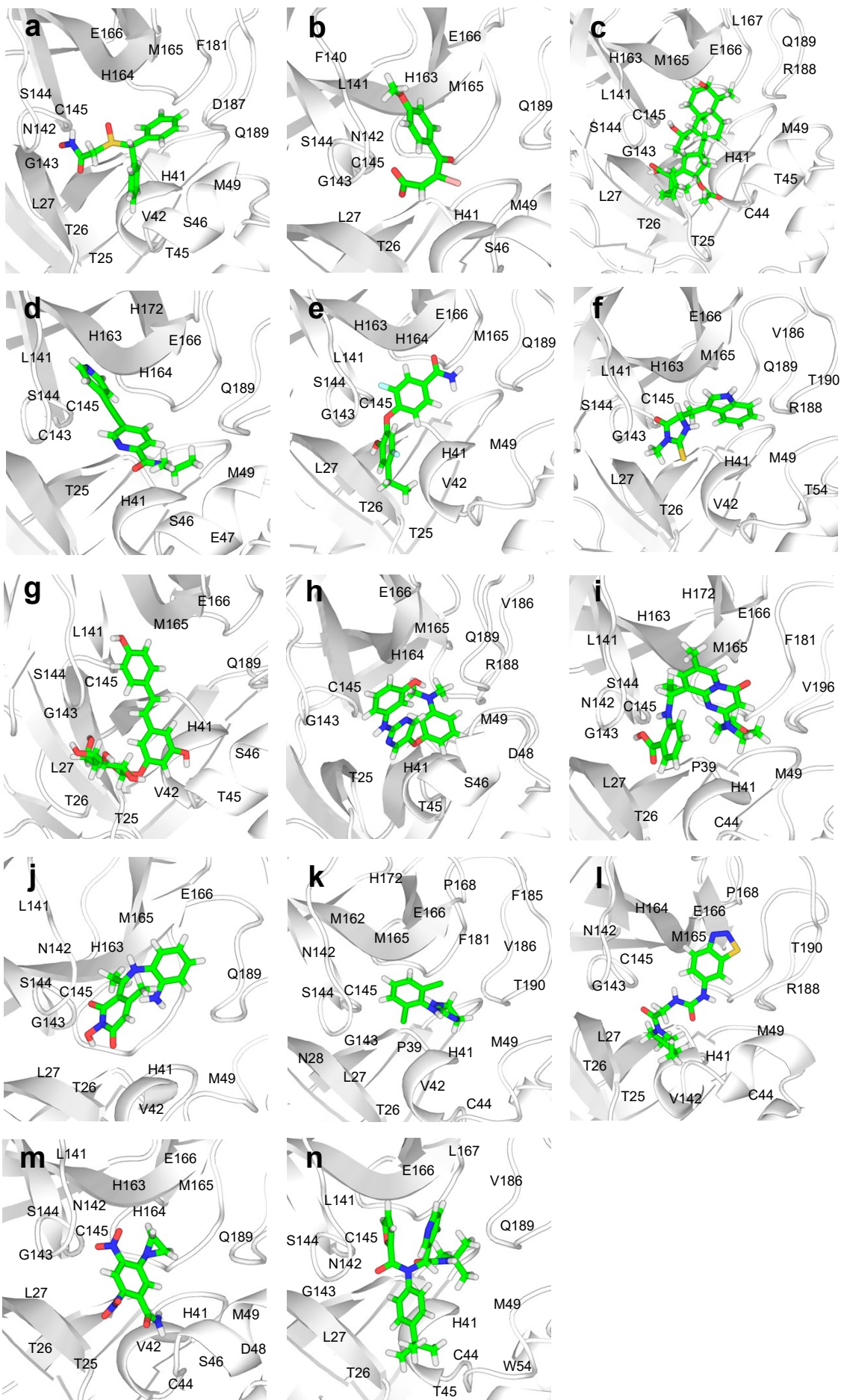


**Fig. S1** Docking of 13 selected compounds and inhibitor ML188 in the pocket of the Mpro: (a) adrafinil; (b) bromebric; (c) Fusidic Acid; (d) LSN-2463359; (e) MUT056399; (f) necrostatin-1; (g) polydatin; (h) polydatin; (i) AZD6482; (j) SUN-B-8155; (k) clonidine; (l) UNC-2327; (m) tretazicar; (n) ML188

## Part 3: Molecular Dynamics Simulations Results and Free-Energy Calculations

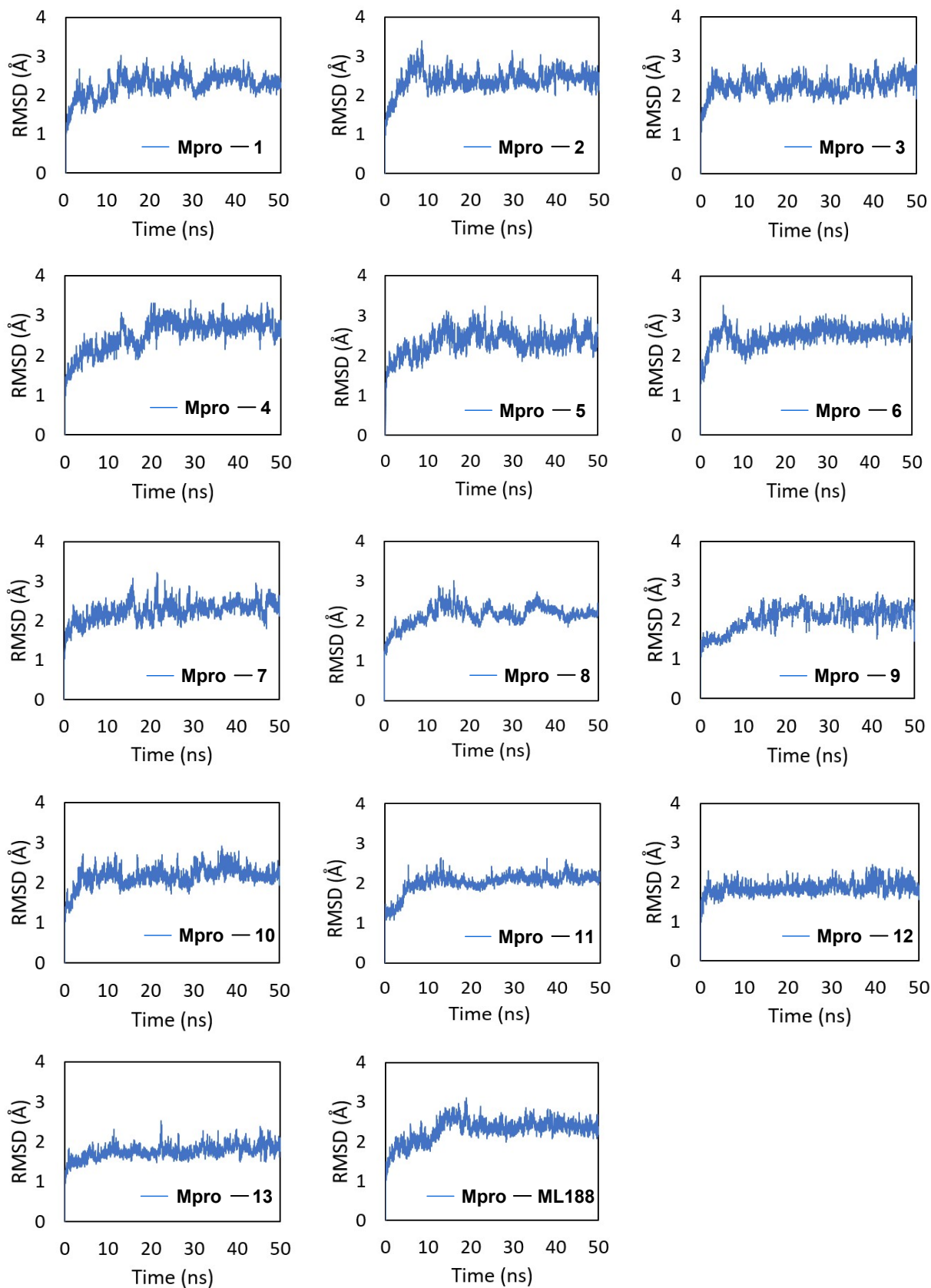


**Fig. S2** Graphical representation of the RMSD for for each ligand in complex with Mpro protein during 50 ns molecular dynamics simulations.

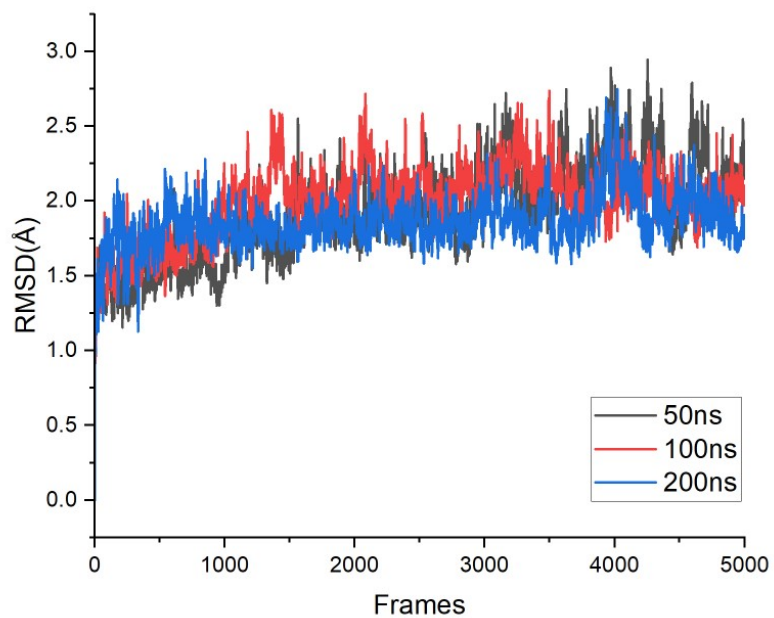


**Fig. S3** Graphical representation of the RMSD during 50 ns, 100 ns and 200ns of MD simulation for compound **12**.

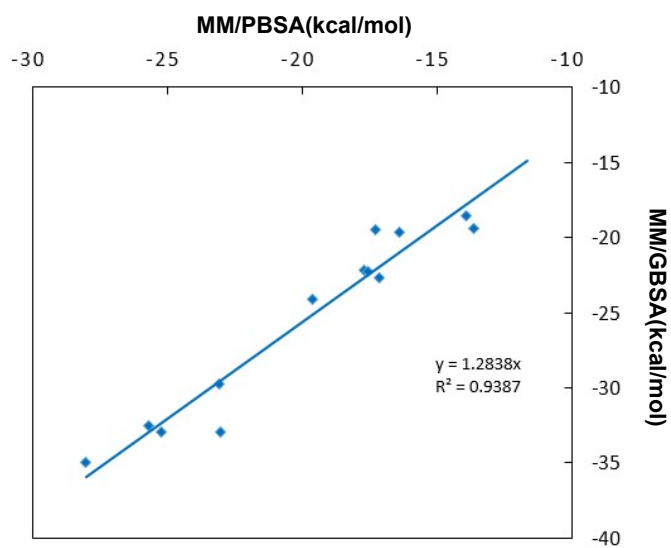


**Fig. S4** The linear relationship between binding energies of  $\Delta G_{\text{MM/PBSA}}$  and  $\Delta G_{\text{MM/GBSA}}$ .

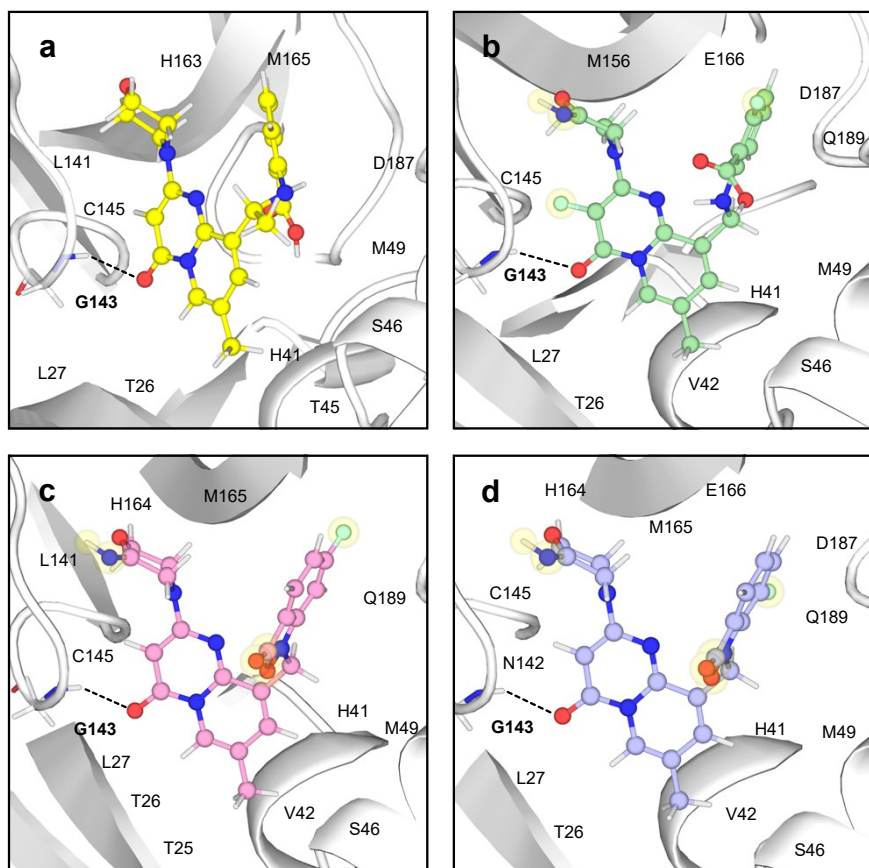


**Fig. S5** Representative snapshot of 3 Mpro-novel ligand complexes. Compared with **9**, the optimized groups in the novel lead compounds are highlighted in yellow sphere.

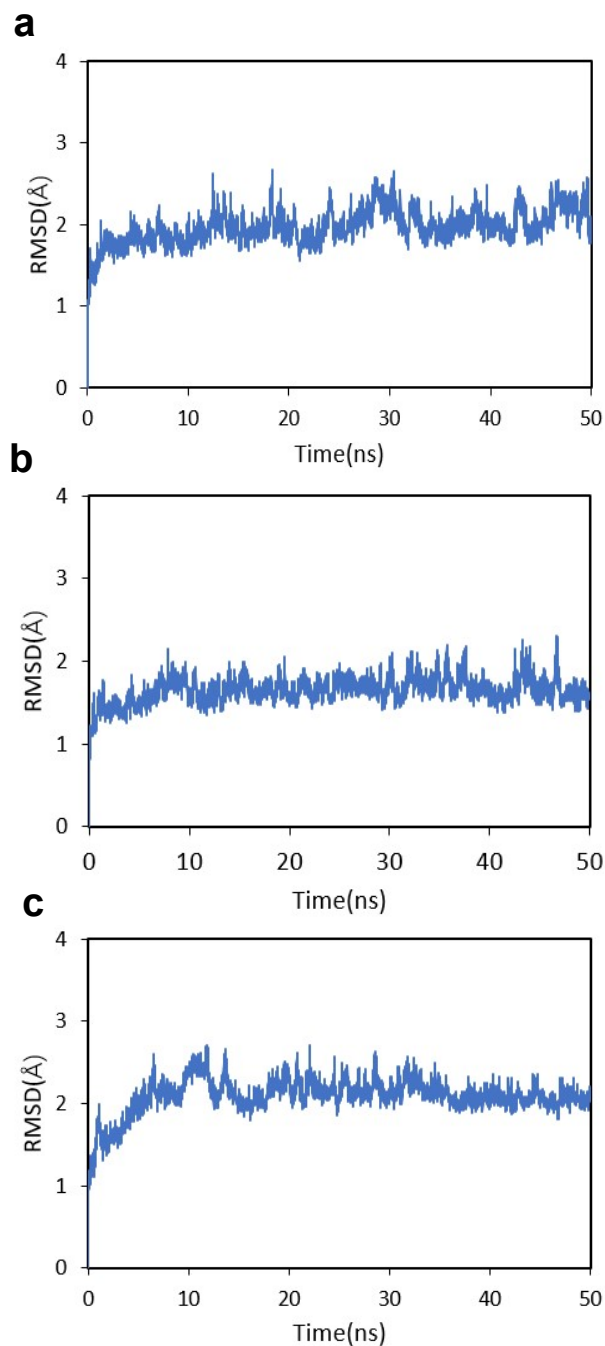


**Fig. S6** Graphical representation of the RMSD during 50 ns of MD simulation for Mpro with lead compound (a) **L1** (b) **L2** (c) **L3** complexes.



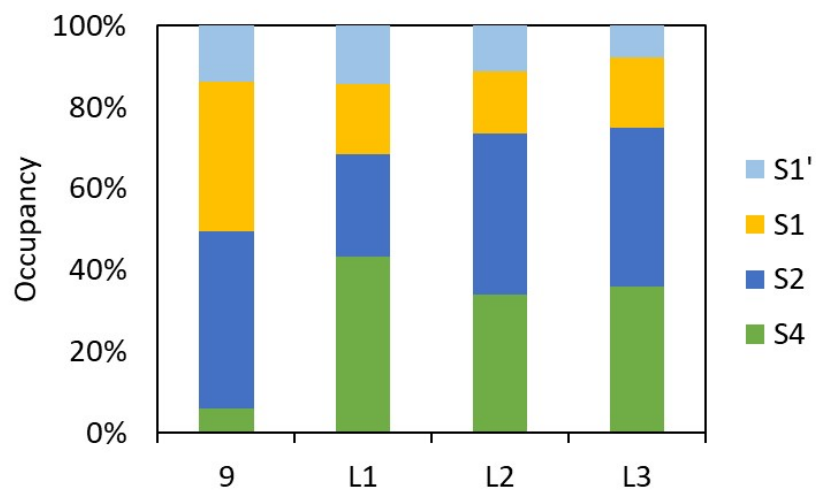


**Fig. S7** Occupancy percentage of compound **9** and three novel lead compound in four subpockets.

**Table S1** Average RMSD values (Å) for 13 selected compounds.

Compound	1	2	3	4	5	6	7	8	9	10	11	12	13	L1	L2	L3
RMSD(Å)	2.5	2.1	2.1	1.8	2.3	2.1	2.4	2.1	1.8	2.2	2.0	2.3	2.0	2.0	1.6	2.1

**Table S2** Relative binding energies of the compound **12** using different frames (energies in kcal/mol).

Frames	$\Delta E_{\text{vdw}}$	$\Delta E_{\text{EEL}}$	$\Delta E_{\text{EPB}}$	$\Delta E_{\text{ENPOLAR}}$	$\Delta G_{\text{MM/PBSA}}$	$\Delta G_{\text{MM/GBSA}}$
50	-41.57	-16.01	30.75	-3.24	-30.08	-38.23
100	-40.43	-13.27	28.68	-3.26	-28.27	-36.11
200	-40.21	-13.60	28.82	-3.24	-28.24	-35.91
500	-40.38	-13.24	28.73	-3.24	-28.13	-35.82

**Table S3** Relative binding energies of compound **12** during 50 ns,100 ns and 200ns of MD simulation (energies in kcal/mol).

Time(ns)	$\Delta E_{\text{vdw}}$	$\Delta E_{\text{EEL}}$	$\Delta E_{\text{EPB}}$	$\Delta E_{\text{ENPOLAR}}$	$\Delta G_{\text{MM/PBSA}}$	$\Delta G_{\text{MM/GBSA}}$
50	-40.43	-13.27	28.68	-3.26	-28.27	-36.11
100	-39.84	-13.99	28.70	-3.18	-28.31	-35.52
200	-39.18	-14.03	28.65	-3.16	-28.06	-34.80

**Table S4** MM/PB(GB)SA binding free energies along with its constituent energies for the selected compounds and three novel lead compounds in eight MD simulations (energies in kcal/mol).

Compound	$\Delta E_{\text{vdw}}$	$\Delta E_{\text{EEL}}$	$\Delta E_{\text{EPB}}$	$\Delta E_{\text{ENPOLAR}}$	$\Delta G_{\text{MM/PBSA}}$	$\Delta G_{\text{MM/GBSA}}$
1	-29.20	-9.07	26.76	-3.03	-14.53	-16.62
	-29.35	-11.72	30.81	-3.07	-13.34	-17.06
	-31.08	-21.80	43.26	-3.07	-12.69	-18.87
	-29.72	-17.75	38.13	-3.09	-12.43	-17.86
	-25.65	-39.50	53.64	-2.98	-14.49	-18.45
	-32.41	-20.10	40.93	-3.19	-14.76	-19.55
	-29.45	-39.01	55.65	-3.17	-15.98	-21.98
	-30.57	-11.81	32.40	-3.15	-13.12	-17.75
2	-23.00	-0.39	11.25	-2.44	-14.58	-18.43
	-23.75	-8.51	6.68	-2.28	-10.83	-15.90
	-22.46	-6.56	19.57	-2.31	-11.76	-19.52
	-24.25	-4.94	10.00	-2.40	-11.71	-17.07
	-11.15	-19.35	17.95	-1.60	-14.15	-17.63
	-24.75	-12.35	23.16	-2.47	-16.40	-24.35
	-25.54	-9.56	20.47	-2.48	-17.12	-23.05
	-24.59	-2.09	16.63	-2.35	-12.40	-19.22
3	-42.45	-6.41	27.57	-4.08	-25.36	-34.43
	-44.69	-2.62	23.05	-4.00	-28.26	-34.03
	-45.97	-5.74	28.53	-4.41	-27.60	-34.66
	-34.40	-9.59	24.43	-3.61	-23.17	-27.01
	-50.96	-1.47	26.91	-4.61	-30.13	-39.46
	-47.67	-6.54	28.46	-4.47	-30.22	-37.91
	-47.59	-5.23	28.71	-4.43	-28.54	-36.87
	-45.59	-1.68	20.88	-4.43	-30.82	-35.57
4	-32.44	-2.97	18.16	-2.67	-19.92	-26.91
	-25.01	-6.48	18.53	-2.41	-15.38	-19.23
	-21.71	-5.22	15.01	-2.11	-14.03	-16.77
	-30.50	-7.63	19.18	-2.76	-21.72	-25.92
	-29.20	-5.20	18.26	-2.74	-18.89	-23.43
	-23.78	-4.37	15.88	-2.34	-14.62	-17.38
	-23.33	-5.42	16.61	-2.22	-14.35	-17.78
	-33.23	-9.68	23.46	-3.31	-22.77	-29.77
5	-27.73	-9.92	24.30	-2.87	-16.23	-18.79
	-30.70	-28.89	44.50	-3.11	-18.20	-27.76
	-21.03	-15.29	22.51	-2.29	-16.10	-17.49
	-32.93	-8.22	23.63	-3.12	-20.63	-24.86
	-31.60	-9.38	27.30	-3.21	-16.89	-23.44
	-28.51	-9.11	21.19	-2.79	-19.23	-24.69

	-29.36	-8.91	24.25	-3.11	-17.13	-21.75
	-24.72	-11.81	23.57	-3.15	-16.11	-19.20
	-32.52	-16.66	30.85	-2.79	-21.12	-26.98
	-29.69	-8.05	22.73	-2.67	-17.67	-22.61
	-25.82	-9.57	23.44	-2.87	-14.81	-19.61
<b>6</b>	-31.36	-14.22	28.17	-2.79	-20.18	-26.38
	-29.74	-10.70	27.02	-2.93	-16.35	-23.06
	-27.08	-12.47	26.53	-2.87	-15.89	-21.40
	-25.06	-8.18	21.18	-2.57	-14.63	-19.25
	-29.57	-7.53	23.66	-2.89	-16.33	-22.04
	-47.81	-17.14	45.51	-4.14	-23.59	-38.28
	-39.43	-9.39	28.48	-3.45	-23.78	-33.50
	-32.56	-10.25	25.91	-3.18	-20.08	-27.39
<b>7</b>	-38.76	-7.88	24.56	-3.55	-25.63	-34.51
	-47.56	-13.61	37.61	-4.05	-27.60	-39.18
	-39.79	-18.46	40.96	-3.82	-21.12	-32.53
	-38.08	-13.93	36.55	-3.80	-19.27	-30.19
	-35.37	-11.39	27.04	-3.40	-23.13	-28.00
	-36.12	-9.71	25.56	-3.23	-23.50	-30.06
	-39.62	-4.47	22.76	-3.52	-24.85	-32.21
	-38.94	-9.23	25.38	-3.44	-26.22	-32.73
<b>8</b>	-37.42	-8.32	24.40	-3.34	-24.68	-31.31
	-37.44	-9.25	24.40	-3.20	-25.50	-31.69
	-38.75	-3.64	21.24	-3.43	-24.58	-31.29
	-44.34	-7.66	26.02	-3.67	-29.65	-36.61
	-41.67	-6.82	25.62	-3.72	-26.60	-34.47
	-42.22	-16.84	39.95	-3.83	-22.93	-29.66
	-48.34	-7.73	31.69	-4.27	-28.65	-36.00
	-38.72	-18.78	40.31	-3.84	-21.04	-27.80
<b>9</b>	-42.91	-13.63	37.83	-3.90	-22.62	-31.18
	-39.96	-12.36	34.37	-3.51	-21.45	-29.20
	-39.54	-11.76	31.92	-4.05	-23.44	-28.77
	-38.71	-12.69	31.48	-3.88	-23.80	-27.61
	-34.04	-26.37	43.52	-3.66	-20.54	-27.83
	-27.92	-13.15	27.11	-2.91	-16.87	-19.47
	-27.21	-11.63	27.28	-2.90	-14.46	-18.62
	-24.09	-11.99	23.48	-2.84	-15.43	-16.75
<b>10</b>	-26.85	-7.57	22.90	-2.78	-14.30	-16.98
	-24.55	-10.97	21.79	-2.58	-16.31	-18.17
	-29.32	-23.33	32.33	-3.03	-23.36	-26.15
	-25.80	-16.71	24.13	-2.82	-21.20	-23.63
	-23.64	-10.06	20.24	-2.74	-16.21	-16.38

<b>11</b>	-29.65	-3.29	18.02	-2.69	-17.61	-25.46
	-27.78	-3.83	13.46	-2.43	-20.59	-24.42
	-27.22	-4.43	15.06	-2.44	-19.03	-23.91
	-26.02	-2.91	11.73	-2.38	-19.58	-22.72
	-27.70	-3.45	11.49	-2.40	-22.06	-25.66
	-24.20	-3.39	12.27	-2.31	-17.64	-21.12
	-26.40	-2.29	12.58	-2.46	-18.57	-23.04
	-28.89	-4.19	13.89	-2.45	-21.65	-26.53
<b>12</b>	-38.44	-7.62	24.58	-3.12	-24.60	-31.02
	-40.43	-13.27	28.68	-3.26	-28.27	-36.11
	-37.21	-8.85	27.26	-3.32	-22.13	-30.41
	-31.46	-11.90	23.20	-3.13	-23.29	-27.11
	-42.59	-18.07	34.55	-3.41	-29.52	-37.42
	-39.44	-16.48	35.29	-3.40	-24.03	-34.38
	-37.62	-7.75	24.69	-3.27	-23.94	-31.62
	-40.21	-18.73	36.30	-3.36	-25.99	-35.50
<b>13</b>	-26.18	-11.87	26.28	-2.55	-14.33	-18.05
	-30.30	-27.38	41.00	-2.54	-19.22	-21.11
	-26.60	-13.65	27.18	-2.64	-15.70	-19.35
	-23.89	-16.86	29.17	-2.50	-14.08	-16.63
	-26.30	-12.68	25.90	-2.53	-15.61	-18.37
	-31.21	-13.82	28.83	-2.59	-18.79	-22.54
	-28.17	-12.40	26.27	-2.75	-17.05	-21.06
	-29.06	-9.95	25.23	-2.49	-16.28	-19.95
<b>L1</b>	-47.60	-13.78	34.60	-4.16	-30.94	-40.74
	-49.48	-16.24	38.52	-4.20	-31.39	-43.32
	-50.58	-14.77	35.65	-4.28	-33.98	-43.15
	-52.83	-14.35	38.20	-4.33	-33.31	-45.11
	-53.15	-16.38	38.48	-4.44	-35.49	-45.29
	-46.38	-15.14	33.62	-4.16	-32.06	-38.52
	-46.39	-15.43	32.79	-3.85	-32.87	-41.42
	-50.90	-15.89	37.97	-4.29	-33.10	-43.90
<b>L2</b>	-44.59	-10.40	31.22	-3.77	-27.55	-38.42
	-52.73	-9.64	34.57	-4.32	-32.12	-44.09
	-53.65	-9.43	34.99	-4.34	-32.42	-44.92
	-50.76	-8.82	32.79	-4.22	-31.02	-42.07
	-49.55	-5.43	28.25	-4.06	-30.79	-40.54
	-47.78	-10.85	34.00	-4.07	-28.70	-39.32
	-51.70	-8.22	33.90	-4.32	-30.34	-41.98
	-45.20	-5.65	27.34	-4.03	-27.54	-36.85
<b>L3</b>	-42.49	-9.25	24.46	-3.39	-30.67	-37.21
	-48.38	-15.55	37.39	-4.14	-30.68	-40.24

---

-51.31	-10.00	31.01	-3.97	-34.27	-45.88
-52.01	-9.46	34.27	-4.35	-31.55	-42.61
-51.54	-12.27	35.56	-4.26	-32.52	-44.03
-54.35	-13.36	36.69	-4.32	-35.33	-47.30
-49.71	-9.84	33.80	-4.13	-29.89	-39.77
-52.53	-10.44	35.57	-4.29	-31.69	-43.45

---

**Table S5** Relative binding energies of compound **12** with entropy contributions during 50ns (energies in kcal/mol).

<b>Frames</b>	$\Delta E_{\text{vdw}}$	$\Delta E_{\text{EEL}}$	$\Delta E_{\text{EPB}}$	$\Delta E_{\text{ENPOLAR}}$	<b>TAS</b>	$\Delta G_{\text{MM/PBSA}}$	$\Delta G_{\text{MM/GBSA}}$
50	-41.57	-16.01	30.75	-3.24	–	-30.08	-38.23
50	-41.57	-16.01	30.75	-3.24	-16.36	-13.71	-21.86
100	-40.43	-13.27	28.68	-3.26	–	-28.27	-36.11
100	-40.43	-13.27	28.68	-3.26	-19.66	-8.61	-16.45

We calculated the atomic partial charges before docking using the AM1-BCC charges and restrained electrostatic potential (RESP). Then their binding energies were calculated separately, and the results were not much different.

**Table S6** Comparison of MM/PB(GB)SA binding free energies assigning AM1-BCC charges and RESP charges for compound **12** (energies in kcal/mol).

Compound	$\Delta E_{\text{vdw}}$	$\Delta E_{\text{EEL}}$	$\Delta E_{\text{EPB}}$	$\Delta E_{\text{ENPOLAR}}$	$\Delta G_{\text{MM/PBSA}}$	$\Delta G_{\text{MM/PBSA}}$
	-38.44	-7.62	24.58	-3.12	-24.60	-31.02
	-40.43	-13.27	28.68	-3.26	-28.27	-36.11
	-37.21	-8.85	27.26	-3.32	-22.13	-30.41
<b>12</b>	-31.46	-11.90	23.20	-3.13	-23.29	-27.11
(BCC)	-42.59	-18.07	34.55	-3.41	-29.52	-37.42
	-39.44	-16.48	35.29	-3.40	-24.03	-34.38
	-37.62	-7.75	24.69	-3.27	-23.94	-31.62
	-40.21	-18.73	36.30	-3.36	-25.99	-35.50
	-38.27	-16.13	33.29	-3.37	-24.48	-31.12
	-37.95	-17.69	31.45	-3.57	-27.75	-32.89
	-36.71	-8.67	26.50	-3.31	-22.19	-30.10
<b>12</b>	-37.20	-9.90	27.10	-3.29	-23.29	-29.48
(RESP)	-37.39	-16.92	31.99	-3.51	-25.83	-31.05
	-33.03	-8.47	22.57	-3.00	-21.94	-26.93
	-35.37	-6.67	24.09	-3.21	-21.15	-26.76
	-32.89	-14.49	28.33	-3.16	-22.21	-27.09



**Table S7** Hydrogen bond interactions in the Mpro-ligand complexes

<b>compound</b>	<b>Hydrogen Bond</b>	<b>Lifetime(%)</b>	<b>Distance(Å)</b>
<b>3</b>	(UNK307)@O5...H-N(G143)	14.78	2.53
	(UNK307)@O5...H-N(E166)	60.22	2.37
<b>8</b>	(UNK307)@O2...H1-OG1(T25)	19.28	2.08
	(UNK307)@O1...HD1-ND1(H41)	85.10	2.67
	(UNK307)@N2-H2...OG(S46)	15.84	2.61
<b>9</b>	(UNK307)@O2...H-N(G143)	53.08	2.35
	(UNK307)@N5-H51...O (L141)	8.04	2.46
<b>12</b>	(UNK307)@O2...H-N(G143)	16.68	2.41
	(UNK307)@O2...H-N(G145)	21.98	2.25

**Table S8** Protein–ligand binding energy decomposition of critical residues involved in the formation of Mpro binding pocket (energies in kcal/mol).

residue	1	2	3	4	5	6	7	8	9	10	11	12	13
T 25	-1.29	-0.10	-1.27	0.01	-1.36	-0.74	-0.92	-1.14	-0.23	-0.45	-0.11	-0.35	-0.43
T 26	-0.07	-0.01	-0.16	0.01	-0.05	-0.26	-0.50	-0.04	-0.01	-0.80	0.00	-0.03	-0.10
L 27	-0.27	-0.24	-0.71	-0.02	-0.40	-0.65	-0.52	-0.24	-0.45	-0.43	-0.37	-0.22	-0.63
P 39	-0.02	-0.04	-0.22	0.00	-0.15	-0.27	-0.12	-0.13	-0.15	-0.05	-0.16	-0.11	-0.10
R 40	-0.06	-0.07	-0.34	0.01	-0.03	-0.44	-0.08	-0.31	-0.25	0.01	-0.21	-0.20	-0.05
H 41	-2.02	-1.25	-1.18	-0.01	-1.65	-2.06	-1.71	-2.24	-1.60	-1.38	-1.48	-1.96	-1.52
V 42	-0.09	-0.01	-0.30	0.00	-0.11	-0.21	-0.10	-0.22	-0.11	-0.07	-0.11	-0.21	-0.18
C 44	-0.29	-0.02	-1.09	0.00	-0.77	-0.51	-0.18	-1.62	-0.81	-0.12	-0.12	-0.40	-0.08
T 45	-1.05	-0.05	-0.88	0.00	-0.33	-0.40	-0.11	-1.84	-1.03	-0.17	-0.07	-0.39	-0.10
S 46	-0.56	-0.17	-1.13	-0.06	-0.68	-0.55	-0.10	-0.97	-0.50	-0.41	-0.30	-0.30	-0.16
D 48	-0.01	0.03	-0.19	0.00	-0.15	-0.07	-0.04	-0.38	-0.26	0.00	-0.06	-0.11	-0.03
M 49	-0.36	-0.64	-1.75	-0.20	-1.71	-1.17	-0.70	-2.75	-2.12	-1.63	-1.52	-1.65	-1.02
P 52	0.00	-0.01	-0.25	0.00	-0.05	-0.09	-0.14	-0.32	-0.17	-0.09	-0.15	-0.03	-0.01
F 140	-0.03	-0.13	0.00	-0.33	0.00	-0.02	-0.12	0.00	-0.24	0.00	-0.01	-0.12	-0.08
L 141	-0.05	-0.26	-0.02	-0.54	0.00	-0.07	-0.16	0.00	-0.27	-0.02	0.00	-0.32	-0.03
N 142	-2.55	-2.34	-0.04	-1.19	0.06	-0.33	-0.39	0.05	-0.97	-0.18	0.02	-0.50	-0.49
G 143	-1.71	-1.36	-0.28	-0.11	0.00	-0.27	-0.19	-0.02	-0.20	-0.20	-0.04	-0.18	-0.50
S 144	-0.83	-0.76	-0.11	-0.40	-0.05	-0.24	-0.15	-0.02	-0.23	-0.05	-0.05	-0.25	-0.47
C 145	-1.46	-1.20	-0.71	-0.22	-0.90	-0.81	-0.63	-0.15	-0.77	-0.48	-0.49	-0.76	-1.17
H 163	-0.51	-0.29	-0.07	-0.48	-0.04	-0.21	-0.09	-0.05	-0.95	-0.07	-0.07	-0.18	-0.29
H 164	-0.13	-0.32	0.16	-0.14	-0.22	-0.30	-0.22	-0.07	-0.22	-0.31	-0.31	-0.92	-0.29
M 165	-0.92	-2.09	-0.86	-1.02	-0.69	-0.84	-1.56	-0.83	-2.25	-1.66	-1.02	-2.70	-1.48
E 166	-0.22	-0.52	0.18	-0.81	0.05	-0.18	-0.18	0.09	-0.41	-0.49	0.03	-0.72	-0.39
L 167	0.04	-0.02	-0.03	-0.18	-0.01	0.00	-0.47	-0.04	-0.17	-0.14	-0.03	-0.06	-0.06
P 168	0.00	0.00	0.02	-0.40	-0.01	0.00	-0.60	0.00	-0.24	-0.08	-0.01	-0.04	-0.03
H 172	-0.11	-0.31	-0.01	-0.40	0.00	-0.05	-0.21	-0.01	-0.26	-0.02	-0.02	-0.17	-0.08
D 187	0.07	-0.20	-0.27	-0.01	-0.46	-0.11	-0.26	-0.02	-0.02	-0.15	-0.77	-0.83	-0.33
R 188	-0.01	-0.25	-0.35	-0.04	-0.69	-0.08	-0.27	-0.37	-0.28	-0.28	-0.23	-0.40	-0.24
Q189	-0.04	-0.46	-0.62	-0.52	-0.35	-0.30	-0.86	-0.41	-0.40	-0.66	-0.53	-0.69	-0.34

**Table S9** Protein–ligand binding energy decomposition of secondary structures (SS) involved in the formation of Mpro binding pocket (energies in kcal/mol).

SS	1	2	3	4	5	6	7	8	9	10	11	12	13
Sheet4	-1.63	-0.35	-2.14	0.00	-1.81	-1.66	-1.94	-1.42	-0.68	-1.68	-0.48	-0.59	-1.17
Helix2	-2.48	-1.38	-3.12	0.00	-2.70	-3.50	-2.19	-4.52	-2.93	-1.61	-2.09	-2.89	-1.94
ASL1	-1.98	-0.85	-4.20	-0.27	-3.69	-2.27	-1.09	-6.26	-4.09	-2.31	-2.10	-2.48	-1.32
Loop1	-6.63	-6.05	-1.15	-2.80	-0.89	-1.74	-1.65	-0.15	-2.68	-0.94	-0.56	-2.13	-2.74
Sheet12	-1.75	-3.24	-0.62	-2.63	-0.91	-1.53	-2.52	-0.89	-4.00	-2.67	-1.40	-4.57	-2.50
ASL2	-0.08	-1.21	-1.24	-1.38	-1.51	-0.53	-2.19	-0.82	-1.19	-1.20	-1.56	-2.14	-1.03

**Table S10** Pocket occupancy of 13 selected compounds and generated 3 novel lead compounds

<b>Compound</b>	<b>S1'</b>	<b>S1</b>	<b>S2</b>	<b>S4</b>
<b>1</b>	29.80%	35.79%	34.64%	-0.23%
<b>2</b>	28.45%	47.98%	16.67%	6.89%
<b>3</b>	27.90%	12.48%	50.48%	9.14%
<b>4</b>	9.21%	63.96%	14.65%	12.18%
<b>5</b>	25.63%	15.84%	45.70%	12.84%
<b>6</b>	30.81%	17.82%	47.04%	4.33%
<b>7</b>	27.11%	29.34%	26.44%	17.11%
<b>8</b>	8.77%	12.92%	72.67%	5.64%
<b>9</b>	13.79%	36.86%	43.38%	5.98%
<b>10</b>	24.34%	27.77%	36.53%	11.36%
<b>11</b>	15.25%	21.95%	45.12%	17.69%
<b>12</b>	14.24%	38.39%	34.06%	13.31%
<b>13</b>	33.52%	29.73%	27.86%	8.88%
<b>L1</b>	14.41%	17.06%	25.14%	43.38%
<b>L2</b>	11.14%	15.40%	39.62%	33.84%
<b>L3</b>	7.91%	17.06%	39.24%	35.79%

## Part 4: Physicochemical properties and ADME analysis

Physicochemical and ADME characteristics of these inhibitors for Mpro, derived using the software SwissADME:

**Table S11** Physicochemical properties of these compounds.

Ligand	MW	Natoms	Nrotb	H-bond acceptor	H-bond donor	Molar Refractivity	TPSA	LogP	LogS	Lipinski
<b>1</b>	289.4	20	6	3	2	77.5	85.6	1.5	-2.8	+
<b>2</b>	285.1	16	4	4	1	61.9	63.6	1.8	-3.0	+
<b>3</b>	516.7	37	6	6	3	146.3	104.1	0.8	-6.1	+
<b>4</b>	265.3	20	3	3	1	77.1	54.9	2.4	-3.1	+
<b>5</b>	293.3	21	4	5	2	72.8	72.6	2.4	-3.7	+
<b>6</b>	259.3	18	2	1	2	81.9	80.2	2.0	-2.9	+
<b>7</b>	390.4	28	5	8	6	100.0	139.8	1.8	-2.9	+
<b>8</b>	322.4	24	5	4	2	94.3	70.5	2.9	-4.2	+
<b>9</b>	408.5	30	5	5	2	117.7	96.2	2.9	-3.7	+
<b>10</b>	273.3	20	2	4	3	78.1	100.8	2.1	-2.0	+
<b>11</b>	230.1	14	2	1	2	67.0	36.4	1.8	-2.4	+
<b>12</b>	319.4	22	6	4	2	88.7	115.5	2.6	-2.5	+
<b>13</b>	252.2	18	4	5	1	67.2	137.7	0.0	-1.4	+
<b>L1</b>	477.4	35	4	8	2	127.0	126.1	2.9	-3.8	+
<b>L2</b>	423.4	31	3	7	1	115.5	105.8	3.0	-3.8	+
<b>L3</b>	423.4	31	3	7	1	115.5	105.8	2.9	-3.8	+

**Table S12** ADME characteristics of these compounds.

Ligand	GI	BBB	P-gp	CYP1A2	CYP2C19	CYP2C9	CYP2D6	CYP3A4	LogKp (cm/s)
1	high	-	+	-	-	-	-	+	-6.91
2	high	+	-	+	+	-	-	-	-6.45
3	high	-	+	-	-	-	-	+	-5.54
4	high	+	-	+	-	-	-	-	-6.35
5	high	+	-	+	+	+	+	-	-5.98
6	high	-	-	+	+	-	-	-	-6.56
7	high	-	+	-	-	-	-	-	-7.95
8	high	+	-	+	+	+	+	+	-5.87
9	high	-	+	-	-	+	-	+	-7.40
10	high	-	-	-	-	-	-	-	-7.80
11	high	+	-	-	-	-	-	-	-6.59
12	high	-	+	-	-	-	-	-	-7.37
13	high	-	-	-	-	-	-	-	-7.85
L1	high	-	+	-	-	+	-	-	-7.49
L2	high	-	+	-	-	+	-	-	-7.68
L3	high	-	+	-	-	+	-	-	-7.68

## Part 5: Simplified Molecular Input Line Entry System

Table S13 SMILES of 13 input compounds.

Compound	SMILES
1	<chem>O=C(CS(=O)C(c1ccccc1)c1ccccc1)NO</chem>
2	<chem>BC(=CC(=O)O)C(=O)c1ccc(OC)cc1</chem>
3	<chem>CC(=O)OC1CC2(C)C(CC(O)C3C4(C)CCC(O)C(C)C4CCC32C)C1=C(CCC=C(C)C)C(=O)O</chem>
4	<chem>CC(C)NC(=O)c1ccc(C#Cc2ccncc2)cn1</chem>
5	<chem>CCc1cc(O)c(Oc2ccc(C(N)=O)cc2F)cc1F</chem>
6	<chem>CN1C(=O)C(Cc2c[nH]c3ccccc23)NC1=S</chem>
7	<chem>OCC1OC(Oc2cc(O)cc(C=Cc3ccc(O)cc3)c2)C(O)C(O)C1O</chem>
8	<chem>CN(C)c1cccc(Oc2cnc(Nc3cccc(O)c3)nc2)c1</chem>
9	<chem>Cc1cc(C(C)Nc2ccccc2C(=O)O)c2nc(N3CCOCC3)cc(=O)n2c1</chem>
10	<chem>CC(=Nc1ccccc1N)c1c(C)cc(=O)n(O)c1O</chem>
11	<chem>Clc1cccc(Cl)c1NC1=NCCN1</chem>
12	<chem>O=C(NCC(=O)N1CCCCC1)Nc1ccc2nmsc2c1</chem>
13	<chem>NC(=O)c1cc(N2CC2)c([N+](=O)[O-])cc1[N+](=O)[O-]</chem>
L1	<chem>Cc1cc(CNc2ccccc(F)c2C(=O)O)c2nc(N3CCOC(=N)C3)c(F)c(=O)n2c1</chem>
L2	<chem>Cc1cc(Cn2oc(=O)c3ccc(F)cc32)c2nc(N3CCOC(=N)C3)cc(=O)n2c1</chem>
L3	<chem>Cc1cc(Cn2oc(=O)c3ccccc(F)c32)c2nc(N3CCOC(=N)C3)cc(=O)n2c1</chem>